Distinct structures and dynamics of chromatosomes with different human linker histone isoforms

Bing-Rui Zhou, Hanqiao Feng, Seyit Kale, Tara Fox, Htet Khant, Natalia de Val, Rodolfo Ghirlando, Anna R. Panchenko, and Yawen Bai

Supplementary Figure S1-7

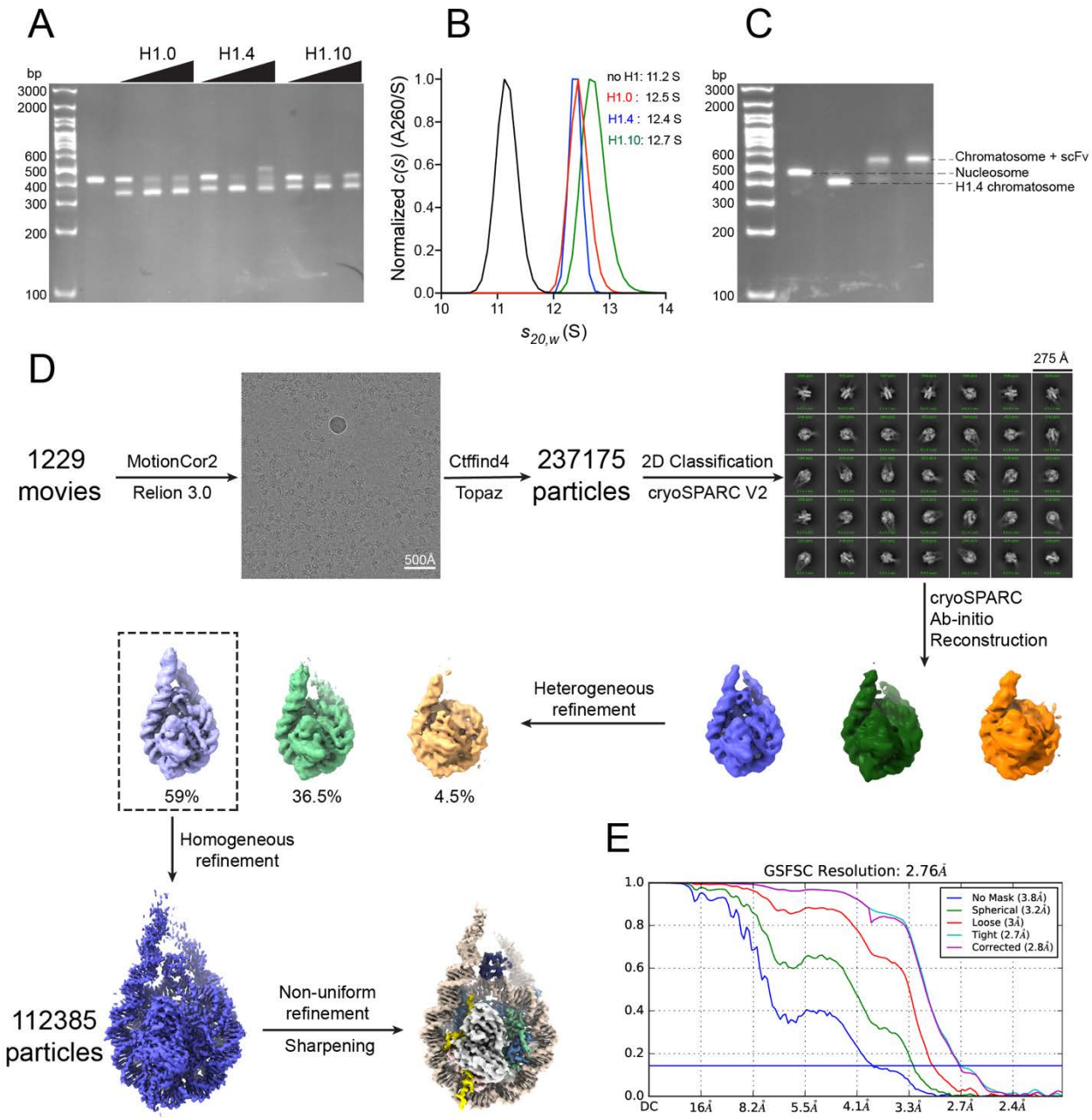

Figure S1. Characterization of chromatosomes and cryo-EM data processing (Related to Figure 1)

(A) Illustration of the determination of the ratio of linker histones over the nucleosome from gel shift experiments.

(B) Characterization of the chromatosomes by sedimentation. The peak intensities were normalized to show different widths of the chromatosomes. The uncertainties for the measured sedimentation coefficients are about 0.05 Svedbergs. The peak values of the three chromatosomes are within the experimental uncertainty but the peak of the H1.10 chromatosome is broader than those of the H1.0 and H1.4 chromatosomes.

(C) Illustration for the binding of the chromatosome containing H1.4 by the scFv. The binding is cooperative; the upper band for the ratio of the chromatosome and scFv is 1:2.
(D) Flow chart illustration for data processing of the H1.4 chromatosome cryo-EM dataset.
(E) FSC curves. The blue straight line is at the value of 0.143.

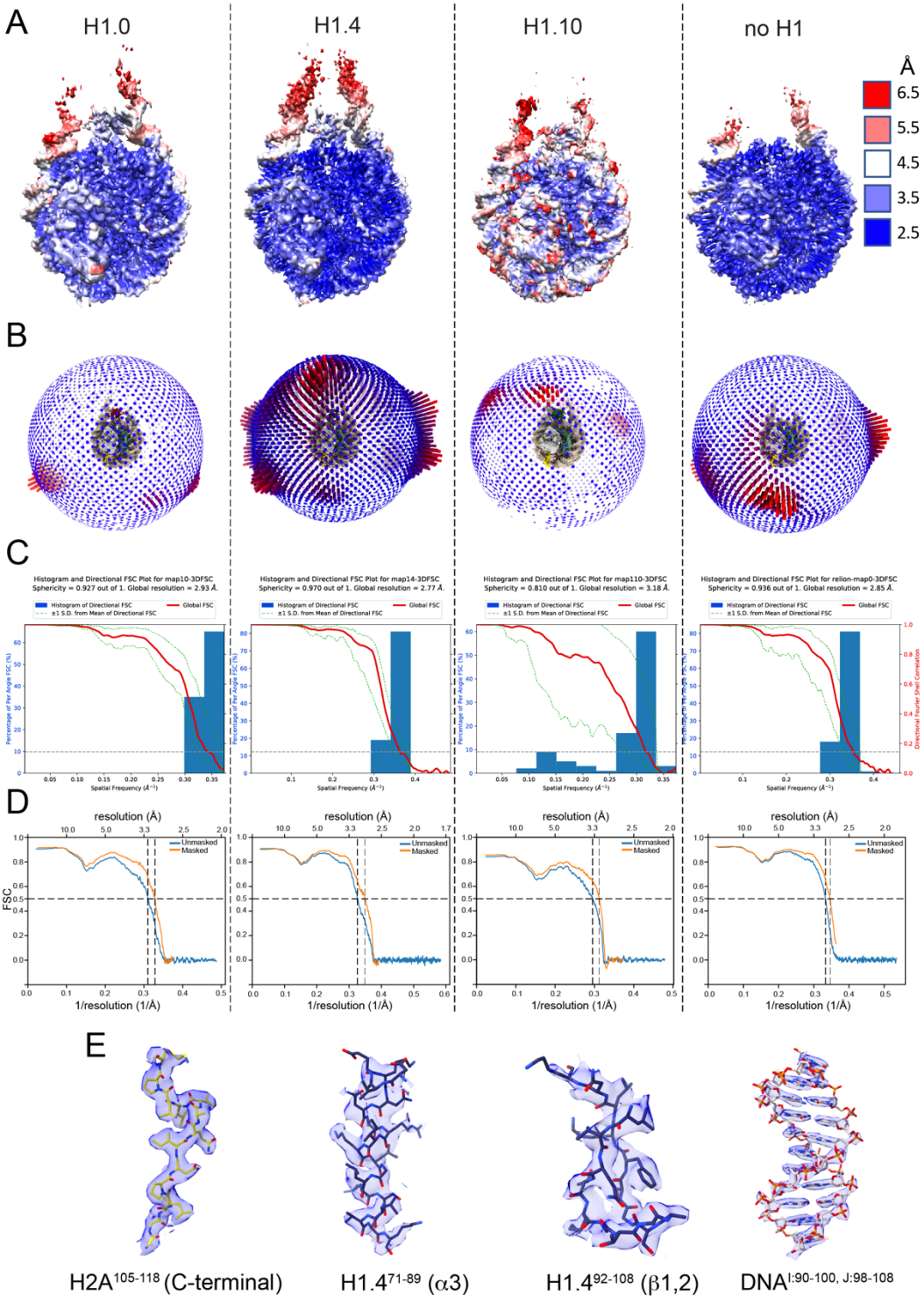

Figure S2. Description of density map quality (Related to Figures 1 and 2)
(A) Local resolution of the density maps.
(B) Angular distribution of particles.
(C) Histograms and directional FSC plots calculated by 3D-FSC.
(D) Model map FSCs calculated using PHENIX.
(E) Examples of typical local density maps with the fitted structural models.

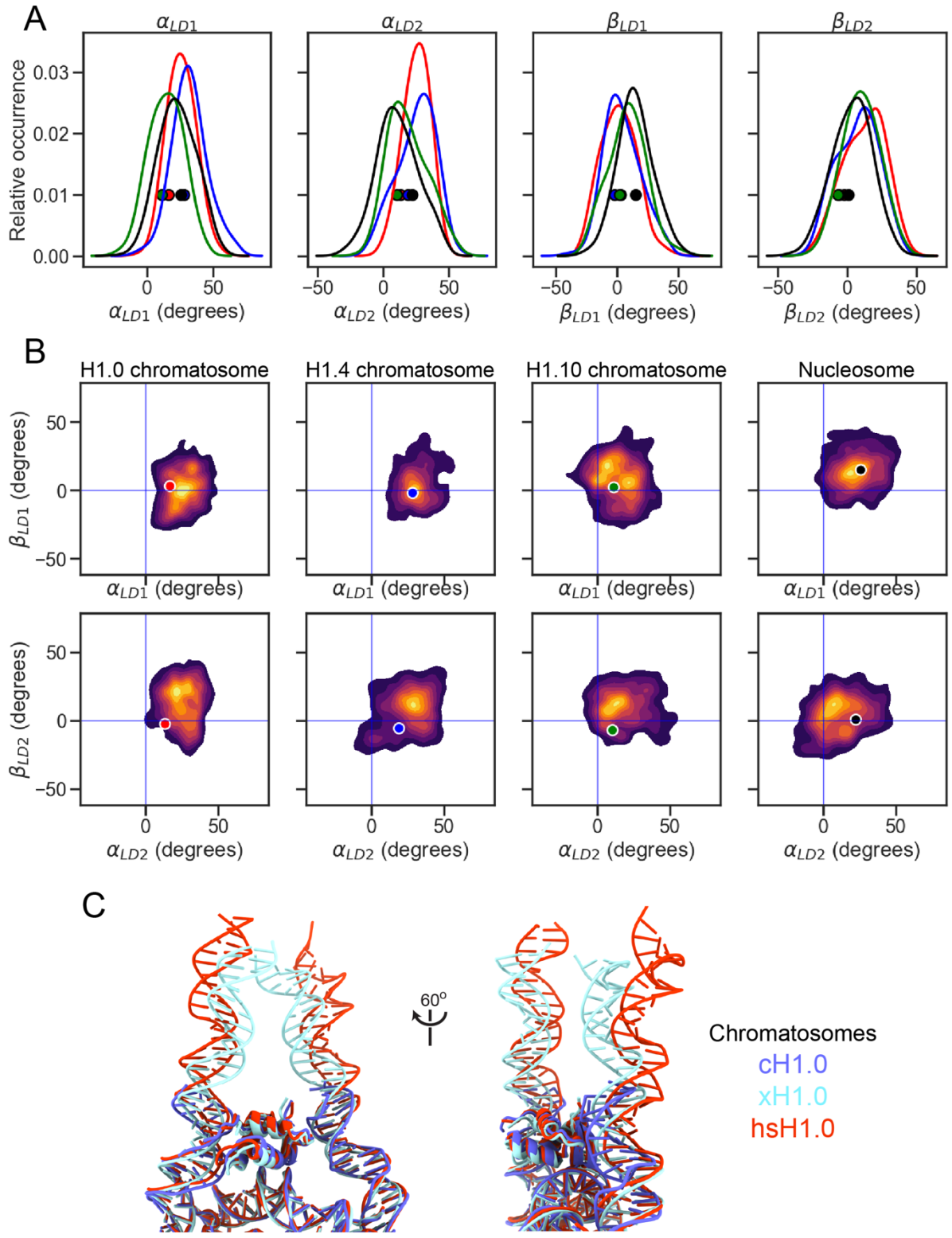
A
α_{LD1}
α_{LD2}
β_{LD1}
β_{LD2}
Relative occurrence
0.03
0.02
0.01
0.00
0
50
−50
α_{LD1} (degrees)
α_{LD2} (degrees)
β_{LD1} (degrees)
β_{LD2} (degrees)
B
H1.0 chromatosome
H1.4 chromatosome
H1.10 chromatosome
Nucleosome
β_{LD1} (degrees)
β_{LD2} (degrees)
C
60°
Chromatosomes
cH1.0
xH1.0
hsH1.0

Figure S3. Linker strand angle distributions and correlation (related to Figure 3)

(A) Distributions of linker strand angles (from left to right): α_{LD1}, α_{LD2}, β_{LD1}, and β_{LD2}. Values of angles for cryo-EM structures are annotated in circles. H1.0 (red), H1.4 (blue), and H1.10 (green) chromatosomes and free nucleosome (black) are shown. Angles are indicated in Figure 3. The dyad base is placed at 0. LD1 is the linker-L1 and LD2 is the linker-α3.

(B) Heatmap distributions of linker strand opening angles of (from left to right) H1.0, H1.4, H1.10 chromatosomes and the free nucleosome. Top panels show the angles for LD1s, bottom panels show the angles for LD2s. Values of angles for cryo-EM structures are indicated in circles. Light blue lines show zero-values for visual assistance.

(C) Comparison of the chromatosome structures containing chicken globular domain of H5 (cH1.0) (pdbID: 4QLC), Xenopus H1.0 (xH1.0) (pdbID: 5NL0) and human H1.0 (hsH1.0) (this work).

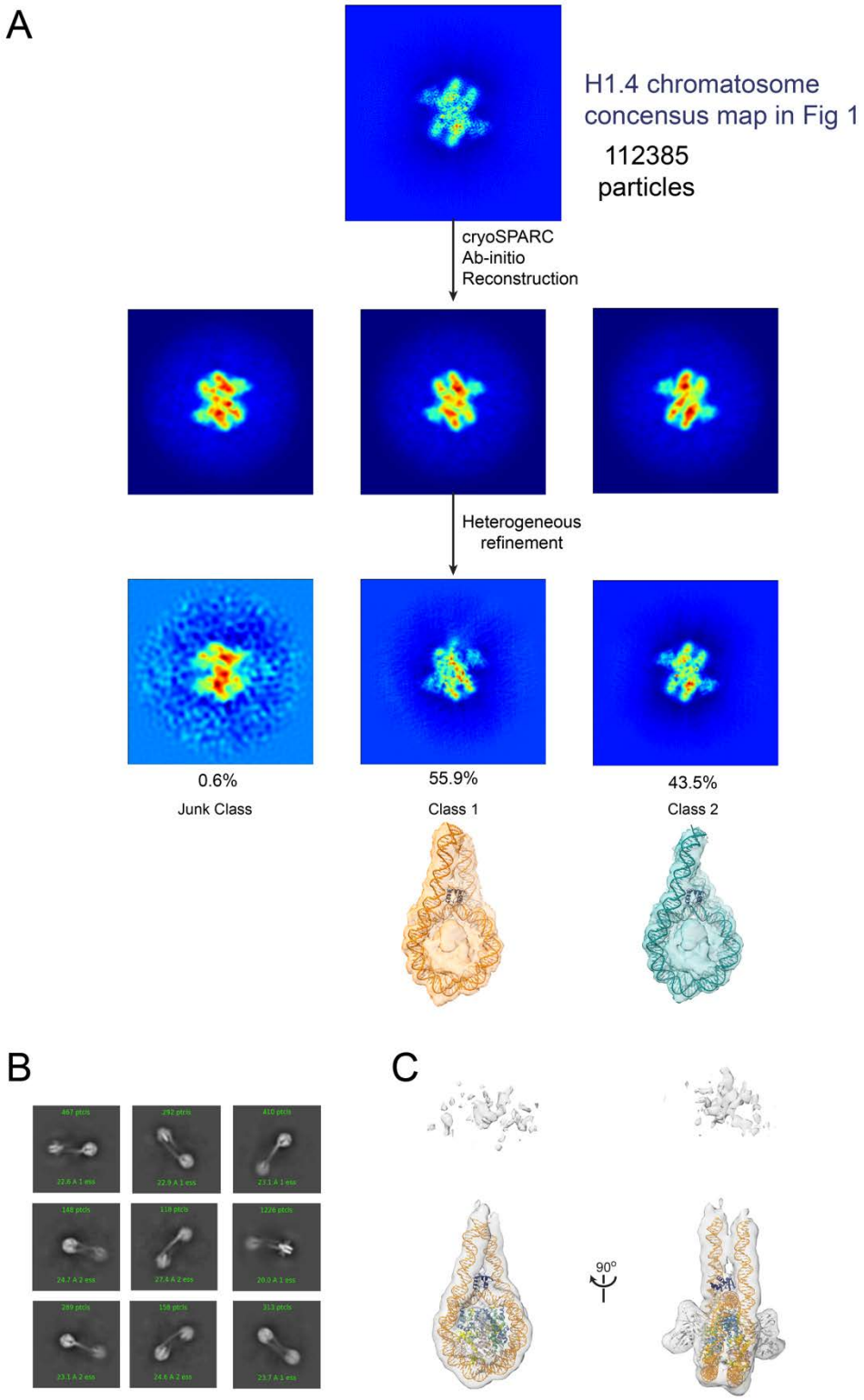

Figure S4. Illustration of the classification of heterogeneous conformations of the H1.4 mono-chromatosome using cryoSPARC and the low-resolution density map of the H1.4 di-chromatosome (Related to Figure 4). (A) 3D classification of the H1.4 chromatosome density map. (B) Representative 2D classification of the H1.4 di-

chromatosome particles. The di-chromatosomes show variable relative orientations. (C) 3D reconstruction of the H1.4 di-chromatosome at ~10 Å resolution, which shows that only one chromatosome in the di-chromatosome display clear density that can be fitted with the mono-chromatosome structure (class 1). The other chromatosome in the di-nucleosome exists in multiple conformations and only show weak density.

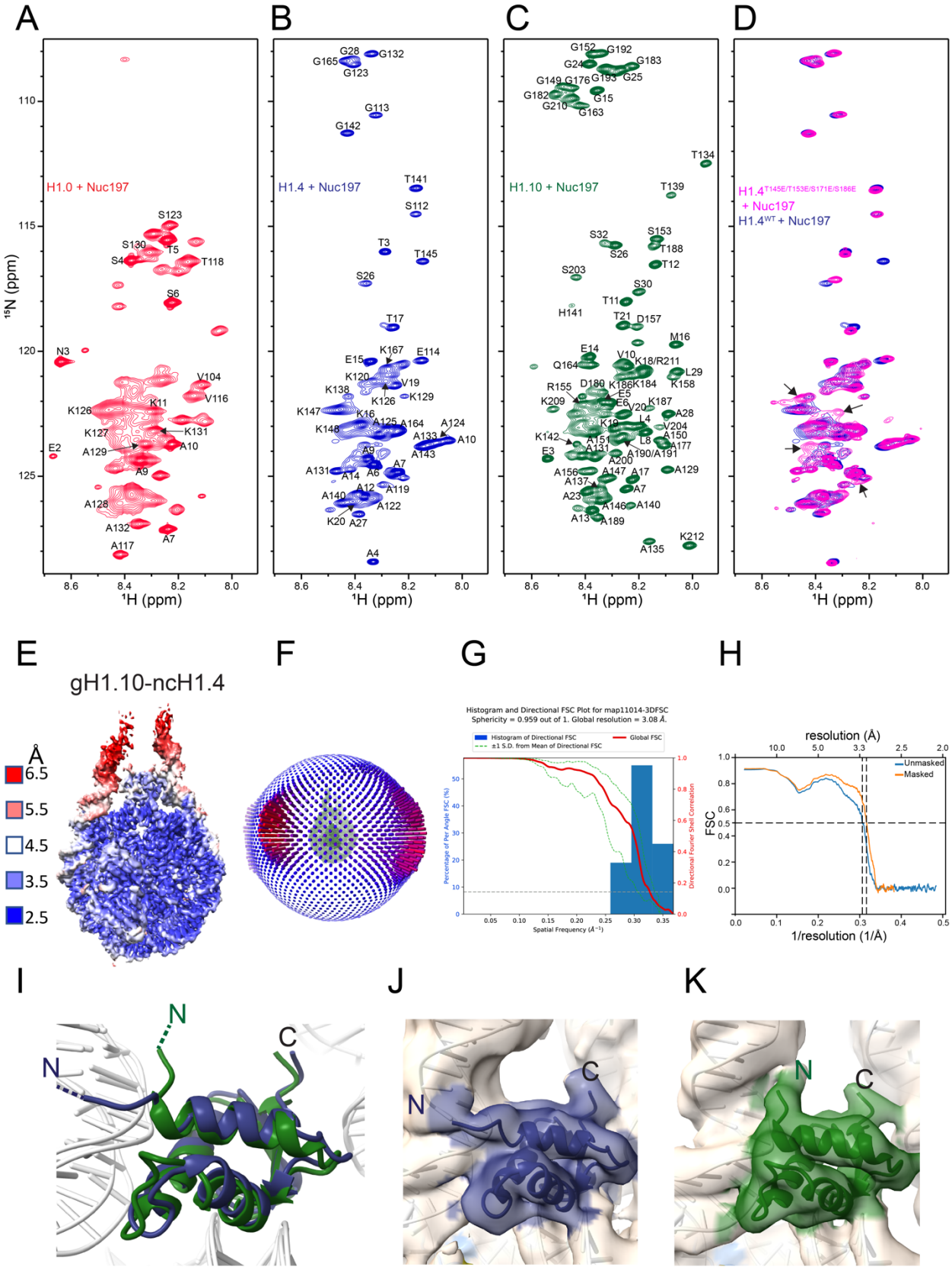
A
B
C
D
H1.0 + Nuc197
H1.4 + Nuc197
H1.10 + Nuc197
H1.4T145E/T153E/S171E/S186E + Nuc197
H1.4WT + Nuc197
15N (ppm)
1H (ppm)
E
gH1.10-ncH1.4
Å
6.5
5.5
4.5
3.5
2.5
F
G
Histogram and Directional FSC Plot for map11014-3DFSC
Sphericity = 0.959 out of 1. Global resolution = 3.08 Å.
Histogram of Directional FSC
Global FSC
±1 S.D. from Mean of Directional FSC
Percentage of Per Angle FSC (%)
Directional Fourier Shell Correlation
Spatial Frequency (Å−1)
H
resolution (Å)
Unmasked
Masked
FSC
1/resolution (1/Å)
I
J
K
N
C

Figure S5. Illustration of the density map quality of the gH1.10-ncH1.4 chromatosome and (Related to Figure 5)

(A-C) ^{1}H-^{15}N HSQC NMR spectra and assignment of linker histone tails H1.0, H1.4, and H1.0 in the chromatosomes.

(D) ^{1}H-^{15}N HSQC NMR spectra of $H1.4^{T145E/T153E/S171E/S186E}$ in the chromatosome (magenta) overlaid with that of H1.4 wild type (blue). Arrows indicate additional peaks observed for this mutant.

(E) Local resolution of gH1.10-ncH1.4 chromatosome cryo-EM map (local resolution for H1.10 globular domain: 3-4.5 Å).

(F) Angular distribution of gH1.10-ncH1.4 chromatosome cryo-EM map

(G) Histogram and directional FSC plot calculated by 3D-FSC.

(H) Model map FSC calculated using PHENIX.

(I-K) Distinct orientations of the N-terminal tails of the H1 isoforms. H1.10 N-terminal tail (green) inserts between the two linker DNA and is close to C-terminal region of the globular domain, whereas the H1.4 (blue) (and H1.0, not shown) N-terminal region extends to the direction that is away from the C-terminal region of the globular domain.

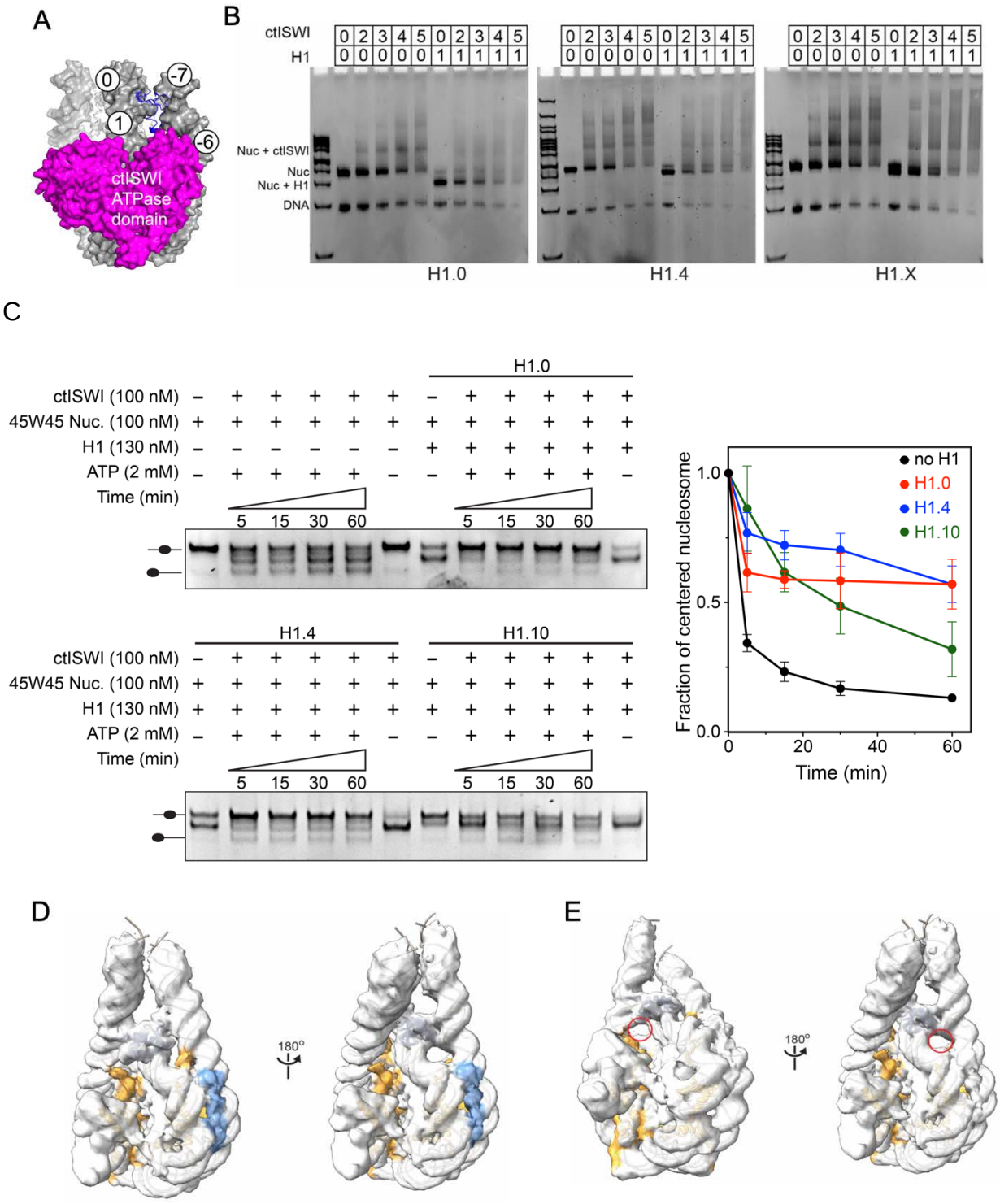

Figure S6. Inhibition of the binding and activity of chromatin remodeler ctISWI by chromatosomes and the ordering of the C-terminal tail of H2A and the N-terminal tail of H3 (Related to Figures 6, 7).

(A) Structure of the nucleosome (grey surface) bound to the ctISWI ATPase domain (magenta) (pdb ID: 6PWF). H3 is shown in ribbon (blue). The numbers indicate the super-helical locations.
(B) ctISWI (ctISWI$_{77\text{-}\Delta\text{-}722}$) bound to the nucleosome, leading to specific bands, whereas when it bound to the chromatosomes, leading to smear image. The number above the gels indicate the molar ratio of the ctISWI or H1 to the nucleosome (100 nM).
(C) Chroamtosomes inhibit the remodeling activity of full-length ctISWI. (Left) Native polyacrylamide gels of the nucleosome sliding assay. The concentration of the ctISWI, nucleosome, linker histones and ATP used are indicated. Reactions were stopped at various times by adding excess amount of plasmid DNA that competitively binds to the ctISWI and linker histones. Note that ctISWI in the absence of ATP appeared to display a chaperone function for linker histones, i.e. enhancing the formation of chromatosomes or preventing dissociation of H1 during electrophoresis. (Right) Fraction of the centered nucleosomes was derived from the gels by measuring band intensity. Error bars indicate standard deviation (n =3) from the mean of three independent experiments. Note that the DNA of the nucleosome consists of 45bp flanking DNA on each end (237bp nucleosome) and W601 sequence in the middle.
(D) Views of the H1.4 chromatosome highlighting both the H2A and H3 N-terminal tails.
(E) Views of the H1.4 chromatosome highlighting the missing of density for the H2A C-terminal end at the linker-$\alpha 3$ side of the chromatosome.

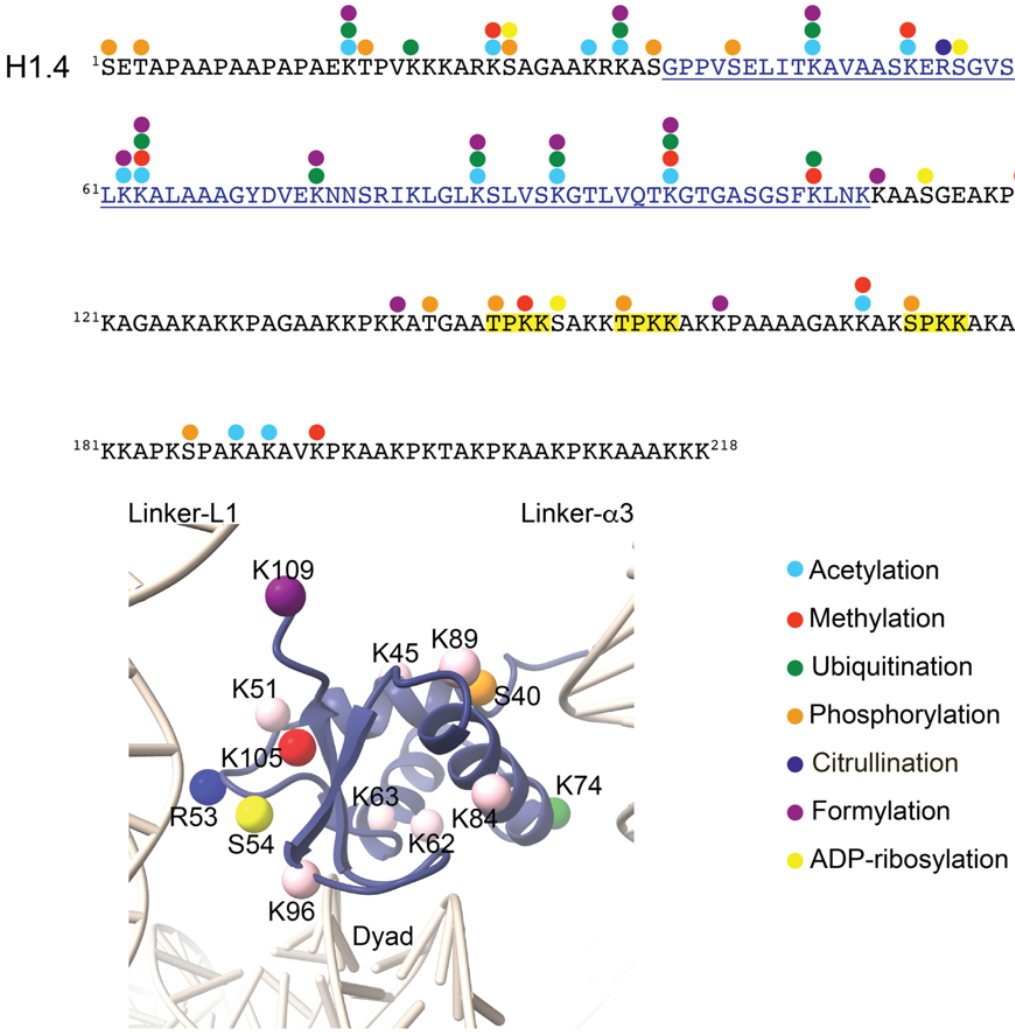

Figure S7. Illustration of known post-translational modifications (PTMs) on human linker histone H1.4 (related to Figure 2). PTM sites in the amino acid sequence of H1.4 (upper panel) and mapping of PTM sites on the globular domain of H1.4 in the chromatosome structure (lower panel). Pink color is used for residues that have more than one modification.